

Changes on optical coherence tomography angiography and fluorescein angiography in eyes with neovascular age-related macular degeneration

So Min Ahn, Mihyun Choi, Cheolmin Yun, Seong-Woo Kim, Jaeryung Oh

Department of Ophthalmology, Korea University College of Medicine, Seoul 02841, Republic of Korea

Correspondence to: Seong-Woo Kim. Department of Ophthalmology, Korea University Guro Hospital 148, Gurodong-ro, Guro-gu, Seoul 08373, Republic of Korea. ksw64723@korea.ac.kr

Received: 2021-08-04 Accepted: 2022-08-26

Abstract

• **AIM:** To evaluate the changes on optical coherence tomography angiography (OCTA) and fluorescein angiography (FA) and their correlation in neovascular age-related macular degeneration (nAMD) before and after intravitreal aflibercept injections (IAIs).

• **METHODS:** In 43 treatment-naïve patients with nAMD, choroidal neovascularization (CNV) in OCTA were morphologically and quantitatively analyzed before and after IAIs to determine whether they are correlated with leakage on FA or not. By combining CNV in OCTA and leakage in FA, lesions were characterized as three types: L+C+ (with both CNV and leakage), L-C+ (with CNV but without leakage), or L+C- lesion (with leakage outside CNV).

• **RESULTS:** Before IAI, while 27 eyes had L+C+ lesion only, 16 eyes had both L+C+ and L-C+ lesions simultaneously. Tiny capillaries and anastomosis in CNV were more developed in L+C+ lesion, at 86.0% and 58.1%, respectively, relative to 9.3% and 9.3% in L-C+ lesions ($P<0.001$). After IAIs in 33 eyes, tiny capillaries and anastomosis were decreased in the lesions with cessation of leakage on FA ($P<0.001$ and $P=0.001$, respectively). In quantitative analysis, neovascularization length and numbers of junctions and endpoints were also significantly decreased.

• **CONCLUSION:** Leakage on FA is associated with CNV morphology in OCTA and remained so after IAIs. Therefore, by carefully assessing the morphological and quantitative changes of CNV in OCTA before and after treatment, activity of nAMD is expected even though CNV on OCTA is not completely matched with fluorescein leakage.

• **KEYWORDS:** choroidal neovascularization; fluorescein angiography; leakage; neovascular age-related macular degeneration; optical coherence tomography angiography
DOI:10.18240/ijo.2022.11.15

Citation: Ahn SM, Choi M, Yun C, Kim SW, Oh J. Changes on optical coherence tomography angiography and fluorescein angiography in eyes with neovascular age-related macular degeneration. *Int J Ophthalmol* 2022;15(11):1837-1844

INTRODUCTION

Neovascular age-related macular degeneration (nAMD) is one of the leading causes of visual impairment in the elderly^[1]. Therefore, diagnosis and management are important to increase quality of life. Dye-based angiography such as fluorescein angiography (FA) and indocyanine green angiography (ICGA) are conventionally the gold-standard imaging modalities by which to diagnose and evaluate nAMD^[2]. More recently, the introduction of optical coherence tomography (OCT) and optical coherence tomography angiography (OCTA) has made it easier to evaluate nAMD in a less invasive fashion^[3-6].

Prior to the development of OCTA, many researchers diagnosed choroidal neovascularization (CNV) according to leakage area on FA and the structural findings on OCT and analyzed the response to treatment based on changes of leakage on FA and the subretinal fluid (SRF) and macular thickness on OCT^[4,7]. After intravitreal anti-vascular endothelial growth factor (VEGF) injection for treatment in nAMD, the presence of leakage and the size of the leakage area on FA were significantly reduced. Typically, eyes without leakage on FA and fluid on OCT after anti-VEGF treatment showed greater improvements in visual acuity than those with both leakage and fluid^[8].

After the recent introduction of OCTA technology, an analysis of OCTA images confirmed that, following treatment of nAMD, the size of the CNV and the density of the neovascularization (NV) complex were reduced with morphologic change of CNV^[5,9-10]. The morphology of CNV was different between the

active and quiescent forms—specifically, active CNV lesions demonstrated greater numbers of small branching vessels and peripheral arcades relative to quiescent CNV^[10-11]. And one of the advantages of OCTA over FA is quantitatively visualized change in retinal microvasculature^[12-13]. In many previous studies, researchers discussed the possibility of replacing invasive FA with noninvasive OCTA^[5,10,14]. However, it is difficult to evaluate the activity of CNV because OCTA does not visualize leakage, limiting its replacement of FA^[6,14].

Therefore, recently, to increase the identification and diagnosis of CNV, FA and OCT were analyzed together with OCTA^[15]. To date, there has been few studies reporting on direct comparison of CNV morphologic characteristics with leakage on FA to evaluate the activity of CNV. In this study, we evaluated the correlation between OCTA and FA images in nAMD both before and after intravitreal aflibercept injection (IAI).

SUBJECTS AND METHODS

Ethical Approval This study was approved by the Institutional Review Board of the Korea University Medical Center in Seoul, Republic of Korea. All data collection and analysis efforts were conducted in accordance with the tenets of the Declaration of Helsinki. Because this was a retrospective study, the Institutional Review Board of Korea University Medical Center waived the need to obtain informed consent from the participants.

Patients To determine eligibility, we reviewed the medical records of treatment-naïve and wet nAMD patients who visited the clinic at Korea University Medical Center between February 2018 and March 2020. In this study, we included patients with exudative nAMD who were aged older than 50y and who received treatment with aflibercept (Eylea; Regeneron Pharmaceuticals, Tarrytown, NY, USA). We excluded any cases with a best-corrected visual acuity less than 20/200; a history of vitreoretinal surgery; any laser treatment administered to the posterior pole of the retina including photodynamic therapy; any prior intravitreal injections; other types of nAMD including polypoidal choroidal vasculopathy and retinal angiomatous proliferation than typical nAMD; or vitreoretinal disease including central serous chorioretinopathy, diabetic retinopathy, epiretinal membrane, retinal vein occlusion, uveitis, and/or high myopia (defined as an axial length of greater than 26.0 mm). Patients with poor auto-segmentation of CNV on OCTA because of large pigment epithelial detachment (PED) or subfoveal hemorrhage were also excluded.

Before treatment with IAI and one month after three loading IVIs, patients underwent best-corrected visual acuity assessment, slit-lamp examination, funduscopy examination, and imaging with FA (Heidelberg Engineering, Heidelberg, Germany) and spectral-domain OCT and OCTA (Heidelberg Spectralis OCT2; Heidelberg Engineering, Heidelberg, Germany).

Image Analysis Acquisition Two independent observers (Ahn SM and Kim SW) classified the AMD status and confirmed

the existence of CNV in each participant through FA, ICGA (Figures 1C, 1D, 2C, and 2D) and OCTA images. ICGA was only used to assess CNV presence and to exclude types other than typical nAMD. These two independent observers confirmed the presence of leakage on FA image and the morphologically qualitative analysis of CNV on OCTA image. In cases of disagreement, the two observers reviewed the cases again and reached a consensus on final decision. FA images in the phase that showed the maximum amount of dye leakage were exported and the presence of dye leakage on FA image was analyzed (Figures 1A, 1B, 2A, 2B, and 3A).

The OCTA instrument used in this study had an acquisition speed of 85 000 A-scans per second (high-speed mode) and 384 A-scans per B-scan. The OCTA scan pattern was 4.3×4.3 mm² (15×15°) centered on the macula. En-face OCTA images were exported from the image viewer software (Heidelberg Eye Explorer, software version 1.21; Heidelberg Engineering, Heidelberg, Germany) following the removal of retinal vessel projection artifacts. The automatic slab from the outer plexiform layer to Bruch's membrane was extracted; if there was segmentation error, the OCTA images that fully included any CNV lesions were extracted by manual adjustment of segmentation (Figures 1E, 1F, 2E, 2F, and 3B). The CNV lesions in extracted OCTA images were clarified by manually selecting CNV and removing artifacts with image cropping, using GNU Image Manipulation Program (GIMP 2.8.14; Figures 1G and 2G).

By assessing the overlaid OCTA image with CNV lesions and fluorescein leakage in FA using the Image J software (version 1.52p; National Institutes of Health, Bethesda, MD, USA), we checked whether the CNV lesions matched with the fluorescein leakage or not (Figures 1A, 1B, 2A, 2B, and 3A). By combining the OCTA and FA images, three lesion presentation types were established: L+C+ lesion (images showing both CNV in OCTA and leakage in FA), L-C+ lesion (images showing CNV in OCTA but without leakage in FA), and L+C- lesion (images showing leakage in FA located outside the CNV).

All CNV lesions were morphologically and quantitatively analyzed based on previous papers^[2,5,9-10,16]. For morphological qualitative analysis of CNV, we distinguished CNV findings of note, including 1) presence of core vessel (defined as large dilated central core vessels in the interior of the lesion extending from the center to periphery); 2) presence of tiny branching capillaries (thin, tangled vessels); and 3) presence of anastomosis (peripheral arcade or inner loops; Figures 1 and 2). In other words, the core vessel was defined as the trunk vessel in the center rather than thin, sprouting, and branching vessels. Tiny branching capillaries were defined as a small vessel that was usually branches off from core vessel and extend to the periphery. Peripheral anastomosis

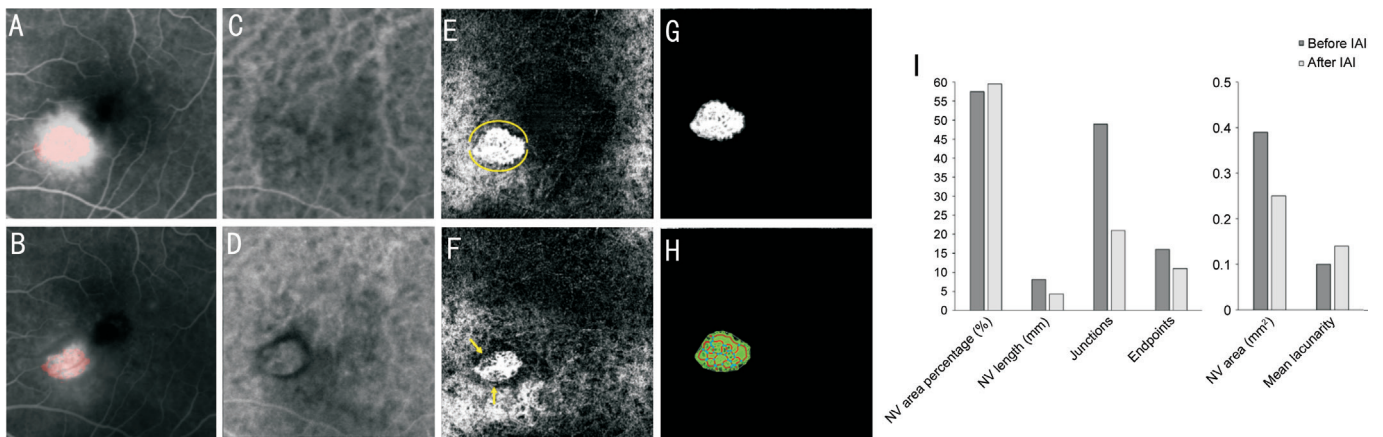


Figure 1 Images of FA leakage and CNV before and after treatment in a patient with L+C+ lesion Before IAI, CNV through OCTA (red color) was matched with FA leakage on FA (L+C+ lesion, A) and CNV was confirmed on ICGA (C). OCTA showed CNV composed of a tangle of small and uniform capillaries and an anastomosis with peripheral arcade (yellow line, E). After IAI, the sizes of the CNV area (red color) and FA leakage were decreased (B), and CNV was confirmed in ICGA imaging (D). The anastomosis was also smaller in OCTA (yellow arrow, F). Projection artifacts were removed in the OCTA image to clarify the CNV lesions using the GNU Image Manipulation Program (G). An open-source software (AngioTool) measured the vessel area surrounded by green lines, the vessel length as indicated by red lines, and the junction number with blue points for quantitative analysis (H). The results of quantitative analysis in this CNV case were 0.39 mm² for NV area, 57.46% for NV area percentage, 8.14 mm for total NV length, 49 total junctions, 16 total endpoints, and 0.10 for mean lacunarity before IAI (I). After IAI, CNV showed reduced total NV length of 4.33 mm, 21 total junctions, and 11 total endpoints, as indicated by quantitative analysis (I). FA: Fluorescein angiography; CNV: Choroidal neovascularization; IAI: Intravitreal aflibercept injection; OCTA: Optical coherence tomography angiography; NV: Neovascularization.

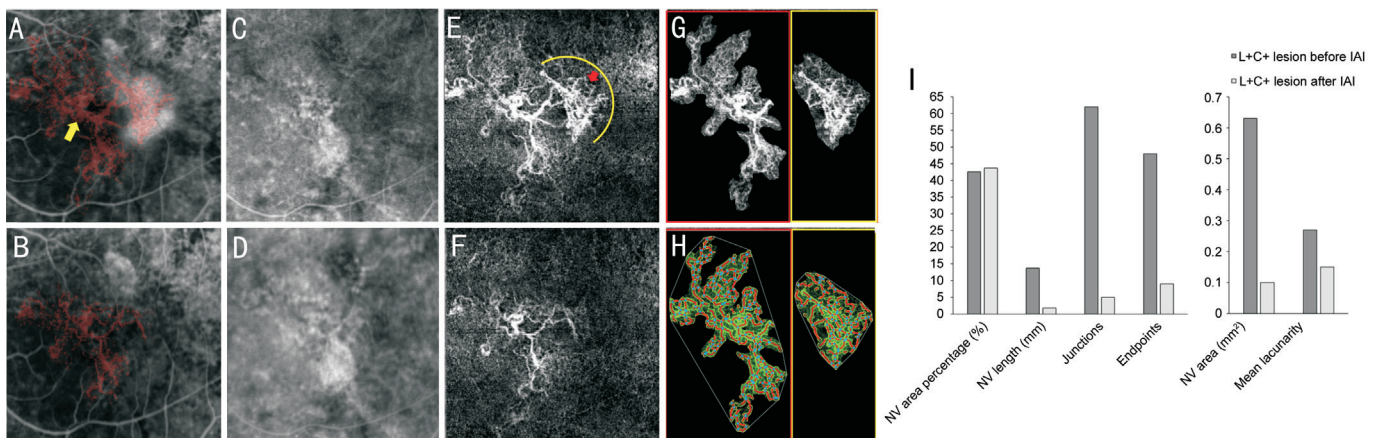


Figure 2 Images of FA and CNV before and after treatment in a patient with CNV composed of both L+C+ and L-C+ lesions In this case, before IAI, there was only a partial leak around the CNV. Some portion of the CNV (red color) was matched with fluorescein leakage on FA image (L+C+ lesion) and residuals of the CNV with a dilated and large core vessel (yellow arrow) were located in the lesion without fluorescein leakage on FA (L-C+ lesion, A). CNV was found on ICGA (C). CNV in the OCTA image composed of the core vessel, tiny capillaries (red arrow), and anastomosis (yellow line, E). After IAI, the size of the CNV area (red color) and the fluorescein leakage were decreased (B), and CNV was found on the ICGA image (D), while tiny capillaries and anastomosis had disappeared (F). However, the core vessel was still remnant despite IAI (F). Projection artifacts were removed in the OCTA image to clarify the CNV lesion using the GNU Image Manipulation Program and CNV lesions were divided into those with fluorescein leakage (yellow box) and those without fluorescein leakage (red box, G). An open-source software (AngioTool) measured the vessel area surrounded by green lines, the vessel length as indicated by red lines, and the junction number with blue points (H). In the L+C+ lesion (yellow box), the results of quantitative analysis in this case were 0.63 mm² for the NV area, 13.67 mm for the total NV length, 62 total junctions, 48 total endpoints, and 0.27 for the mean lacunarity (I). After IAI, CNV in the L+C+ lesion showed with a decreased total NV length of 1.79 mm, five total junctions, and nine total endpoints as indicated by quantitative analysis (I). In the L-C+ lesion (red box), the results of quantitative analysis were 1.43 mm² for the NV area, 31.10 mm for total NV length, 169 total junctions, 83 total endpoints, and 0.51 for mean lacunarity. FA: Fluorescein angiography; CNV: Choroidal neovascularization; IAI: Intravitreal aflibercept injection; OCTA: Optical coherence tomography angiography; NV: Neovascularization.

was defined as the morphology of the peripheral margin of the CNV indicating the connection of adjacent vessels, such as an arcades or loops. For quantitative assessment of CNV, we used the validated and open-source software program *AngioTool* (v0.6a, National Cancer Institute, Center for Cancer Research, Bethesda, MD, USA) with the threshold parameters: 30 and 255, vessel thickness: 5, and removal of small particles: 80 in accordance with previous studies^[11,16]. After optimizing the parameters, the software analyzed the various aspects of vessel network architecture as shown in Figure 1H and Figure 2H, which included: 1) explant area (the area occupied by the convex hull containing the vessels); 2) NV area (the area of the segmented vessels); 3) NV area percentage (percentage of NV area/explant area); 4) total number of junctions (number of junctions in segmented vessels); 5) total number of endpoints (the number of open-ended segments); 6) total length of the vessel (the sum of Euclidean distances between the pixels of all vessels in the image); and 7) mean lacunarity (vessel non-uniformity among all-sized boxes)^[16-17]. A junction was defined as the point of anastomotic connections of two or more vessels in a vascular network. An endpoint was defined as the point of end in branching vessels sprouted without anastomosis. Since a lacunarity was defined as vessel nonuniformity, an increase in lacunarity indicated an inhomogeneous vascular network, and a decrease in lacunarity indicated homogeneity of the vascular network^[16-17].

OCT images were used to assess the presence of subretinal hyperreflective material (SHRM), intraretinal fluid (IRF), SRF, and PED in L+C- lesions (Figure 3C and 3D)^[18]. PED was divided into flat irregular or non-flat irregular.

Statistical Analysis A comparison of variables between the two groups was performed with an independent *t*-test, paired *t*-test, or Mann-Whitney *U* test for continuous variables. For a comparison of categorical variables between the two groups, when the number of variables was greater than five, the Chi-squared test was applied; when the number of variables was less than five, Fisher's exact test was applied. Statistical analysis was performed using the Statistical Package for the Social Sciences software program version 20.0 for Windows (IBM Corporation, Armonk, NY, USA), and *P*-values less than 0.05 were considered to be statistically significant.

RESULTS

A total of 43 eyes of 43 patients (30 males) with a mean age of 70.12±8.59y was included. Thirty-three eyes received a loading dose of three IAIs over three months. The mean best-corrected visual acuity was 0.39±0.26 logMAR before and 0.32±0.34 logMAR after the three loading IAIs (*P*<0.001), while the central retinal thickness was 369.53±127.96 μm before and 242.76±85.60 μm after the three loading IAIs (*P*<0.001). All of the 43 eyes included had CNV and, while

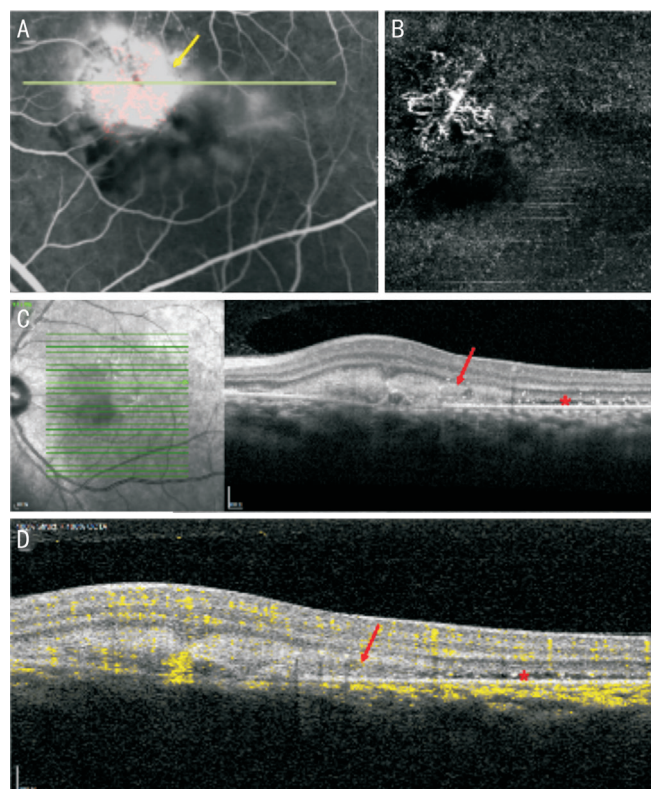


Figure 3 Images of OCT and OCTA in a case of L+C- lesion before treatment CNV (red color) was matched with fluorescein leakage in FA image (L+C+ lesion), but there was also a portion of fluorescein leakage wherein CNV was not detected in OCTA (L+C- lesion, yellow arrow, A). OCTA showed CNV composed of the core vessel, tiny capillaries, and anastomosis with loop (B). In the OCT image, SHRM (red arrow) and shallow SRF (red asterisk) were found in a L+C- lesion (C). The green line on FA image indicates the plane where the OCT image was exported (A, C). An OCT B-scan image on OCTA shows the flow signal as a yellow color and SHRM without flow signal (red arrow) and SRF (red asterisk) at the same location as in Figure 3C were noted (D). FA: Fluorescein angiography; CNV: Choroidal neovascularization; OCT: Optical coherence tomography; OCTA: Optical coherence tomography angiography; NV: Neovascularization; SHRM: Subretinal hyperreflective material; SRF: Subretinal fluid.

27 eyes had only L+C+ lesion, 16 had both L+C+ and L-C+ lesions. Among 43 eyes, 29 eyes had type 1 CNV, 9 eyes had type 2 CNV and 5 eyes had mixed types of type 1 and type 2 CNV. The 44.8% eyes with type 1 CNV had L-C+ lesion, 33.3% eyes with type 2 CNV had L-C+ lesion, and eyes with mixed type had no L-C+ lesion (Table 1).

Comparing the morphologic features of CNV on OCTA between L+C+ and L-C+ lesions in all patients, tiny capillaries and anastomosis were more frequently detected in those patterns with fluorescein leakage (Table 1 and Figures 1 and 2). Mean lacunarity in the quantitative analysis of CNV was significantly higher in L-C+ lesions (Table 1 and Figures 1 and 2). In the

Table 1 Morphological and quantitative analyses of CNV characteristics between L+C+ and L-C+ lesions in all patients (n=43) before treatment

Parameters	L+C+ lesion	L-C+ lesion	P
Types of CNV, n (%)			
Type 1/type 2/mixed	55.2%/66.7%/100.0% (16/6/5)	44.8%/33.3%/0 (13/3/0)	0.067 ^a
Morphologic features, n (%)			
Core vessel	15 (34.9)	12 (27.9)	0.486 ^a
Tiny capillary	37 (86.0)	4 (9.3)	<0.001 ^a
Anastomosis	25 (58.1)	4 (9.3)	<0.001 ^a
Quantitative analysis			
NV area (mm ²)	0.72±0.68	0.47±0.48	0.066 ^b
NV area percentage (%)	43.81±6.71	40.94±11.97	0.246 ^b
Total NV length (mm)	16.42±16.62	10.69±11.24	0.091 ^b
Total No. of junctions	83.23±92.14	58.81±61.57	0.219 ^b
Total No. of endpoints	56.00±56.77	32.44±32.55	0.079 ^b
Mean lacunarity	0.21±0.08	0.43±0.39	0.004 ^b

^aConsidered to be significant when $P < 0.05$; when the number of variables was more than five, the Chi-squared test was applied vs when the number of variables was less than five, Fisher's exact test was applied; ^bIndependent t -test, $P < 0.05$ was considered to be statistically significant. CNV: Choroidal neovascularization; NV: Neovascularization.

subgroup analysis considering both L+C+ and L-C+ lesions ($n=16$), tiny capillaries was more frequently detected in those with fluorescein leakage (81.2% in L+C+ lesions vs 25.0% in L-C+ lesions, $P=0.004$; Figure 2).

Among the total of 43 eyes with CNV with FA leakage, 25 had L+C- lesions. In OCT of L+C- lesions, 20.0% with flat irregular PED, 20.0% with non-flat irregular PED, 56.0% of SHRM without flow signal, 32.0% of IRF, and 32.0% SRF were found on OCT (Figure 3).

After three loading IAIs, tiny capillaries and anastomosis were significantly reduced among lesions with decreased fluorescein leakage and only core vessels showed no significant changes relative to baseline (Table 2 and Figures 1 and 2). By quantitative analysis, NV area, total NV length, total number of junctions, and total number of endpoints were significantly decreased after the three loadings (Table 2, Figures 1 and 2). Mean lacunarity showed a significant increase after the three loading IAIs (Table 2).

DISCUSSION

In this study, changes on OCTA and FA and the correlation between the morphology of CNV in OCTA and fluorescein leakage in FA images were qualitatively and quantitatively analyzed in nAMD patients before and after IAI. Our results indicated that some eyes in nAMD patients presented with CNV lesions on OCTA that overlapped exactly with the area of fluorescein leakage, while in others, the CNV lesions did not exactly match with the area of fluorescein leakage. The characteristics of CNV were morphologically and quantitatively different according to the leakage status in FA. There are several multimodal image tests for diagnosing nAMD and seeing treatment response. FA and ICGA have been conventionally the gold-standard imaging modality, and recently,

Table 2 Changes in CNV characteristics between before and after three loading IAIs in L+C+ lesion by morphological and quantitative analysis

Parameters	Before IAI	After 3 loading IAIs	P
Morphologic features, n (%)			
Core vessel	14 (42.42)	11 (33.33)	1.000 ^a
Tiny capillary	28 (84.85)	7 (21.21)	<0.001 ^a
Anastomosis	21 (63.64)	3 (9.09)	0.001 ^a
Quantitative analysis			
NV area (mm ²)	0.84±0.73	0.53±0.48	0.001 ^b
NV area percentage (%)	42.83±7.10	42.46±9.74	0.805 ^b
Total NV length (mm)	19.32±17.91	12.50±12.34	0.002 ^b
Total No. of junctions	97.52±100.55	65.67±74.41	0.012 ^b
Total No. of endpoints	65.45±61.35	39.88±38.28	0.001 ^b
Mean lacunarity	0.21±0.08	0.26±0.13	0.013 ^b

^aConsidered to be significant when $P < 0.05$, when the number of variables was more than five, the Chi-squared test was applied vs when the number of variables was less than five, Fisher's exact test was applied; ^bPaired t -test, $P < 0.05$ was considered to be statistically significant. IAI: Intravitreal aflibercept injection; NV: Neovascularization.

OCTA has been widely used in eyes with nAMD^[2-5]. However, because the techniques of these imaging tests are different each other, there are many studies comparing the results of these tests with each other. In several previous studies, the size and activity of the CNV did not exactly match one another in imaging modalities such as FA, ICGA, and OCTA^[14,19]. FA is useful for detecting CNV activity by assessing dye leakage^[20]. However, the vascular structure can be concealed by leakage of fluorescein or the visualization of fluorescein can be blocked by the presence of subretinal hemorrhage. ICGA, which can penetrate the retinal pigment epithelium (RPE) and choroid using longer and near-infrared wavelengths, is better than FA

for detecting CNV. The active area in ICGA and FA could be different and the size of CNV in ICGA was sometimes larger than the leakage in FA when subretinal hemorrhage or a large quantity of SRF was located with hypofluorescence. Also, the leakage on FA could extend beyond than the size of the CNV in ICGA when the activity of nAMD is great because ICGA does not show leakage from the CNV and does not reveal the activity of CNV or exudation^[21]. Recently, with the development of OCTA, the morphology of CNV can be visualized more effectively in OCTA^[22]. However, dynamic dye leakage from CNV cannot be seen on OCTA, similar to on ICGA. Therefore, the comparison of OCTA and FA might yield similar results to the comparison of ICGA and FA mentioned previously. There are few reports about the comparison of CNV size between OCTA and FA^[14,19]. Further, there is few reports discussing the morphological comparison of OCTA and FA by directly overlapping the two types of images. In this study, we found that CNV lesions did not always match with the area of fluorescein leakage and the characteristics of CNV were also morphologically and quantitatively different according to the leakage status in FA.

The size and morphology of CNV in OCTA were analyzed for conducting comparison between active and quiescent CNV or determining the response to anti-VEGF treatment^[5,9-11]. Active CNV lesions often had a prominent central vessel and greater numbers of small branching vessels and peripheral arcades in comparison with quiescent NV. Especially, Coscas *et al*^[5] reported that the presence of tiny branching vessels and a peripheral anastomotic arcade are predictive biomarkers of CNV activity on OCTA. They noted tiny branching vessels in 82.5% of the cases, vascular loops in 81.7%, and peripheral anastomotic arcades in 66.7%. Similarly, in this study, tiny capillaries (86.0%) and anastomosis including vascular loop and peripheral anastomotic arcades (58.1%) were frequently paired with lesions with fluorescein leakage. Because tiny capillaries and anastomosis were more concentrated in lesions with fluorescein leakage than in those without fluorescein leakage, suggesting homogeneous CNV in OCTA, the mean lacunarity was significantly lower in lesions with fluorescein leakage. After IAI, not only were tiny capillary and anastomosis morphologically decreased but also total NV length, total number of junctions, and total number of endpoints were quantitatively reduced in this study. A decrease of junction or endpoint presented a decrease of vascular network^[23]. The lacunarity presenting vascular non-uniformity was high in L-C+ lesion (CNV without leakage) or after IAI, because the relatively irregular branching capillaries decreased and only large vessels or core vessels remained, indicating uniformity. Therefore, an increase in lacunarity might show that the activity of CNV is small or stable^[16]. These results

suggest the association between morphologic features of CNV and quantitative analysis of CNV. The CNV network could be quantitatively analyzed using the AngioTool software program. The activity of CNV was evaluated between the active and quiescent states or good and poor responses in some previous studies^[11,16]. However, no study has assessed the quantitative change in the CNV network between before and after anti-VEGF injection using the AngioTool software program; further, we analyzed quantitative features of CNV matched with fluorescein leakage using the AngioTool software program.

In this study, unlike tiny capillaries and anastomosis, the presence of core vessels was not different between the lesions with fluorescein leakage and those without fluorescein leakage prior to IAI. In addition, the core vessels remained unchanged after IAI. The size and density of CNV were reduced after anti-VEGF treatment in type 1 or type 2 CNV but the central vessel trunk remained unchanged and resistant to anti-VEGF treatment^[24]. Elsewhere, large prominent vessels were not changed by anti-VEGF treatment, while tiny vessels were attenuated and reduced^[5]. The results confirmed that large prominent vessels like core vessels did not demonstrate CNV activity. Although the presence of CNV on OCTA was highly correlated with the presence of fluorescein leakage that demonstrated the clinical activity of CNV, the clinical activity varied according to the morphologic characteristics of CNV on OCTA^[25]. Therefore, CNV on OCTA was not exactly matched with fluorescein leakage and we highlighted differences in CNV morphology between L+C+ and L-C+ lesions.

We analyzed whether leakage on FA image and the CNV on OCTA image were matched through overlaid images of FA and OCTA; we identified an L+C- lesion. Therefore, we evaluated the features of OCT in L+C- lesion and SHRM, IRF, and SRF were usually detected in L+C- lesion. The presence of fluid in the retinal, subretinal, and sub-RPE spaces demonstrated exudation of nAMD and could reveal dye leakage on FA^[26-27]. SHRM, IRF, and SRF were predominantly found in L+C- lesions and could be presented without CNV. These lesions showed the large leakage on the FA compared to the actual CNV. Especially, nonvascularized SHRM was observed in 56.0%. Giani *et al*^[28] reported that SHRM and SRF were more significantly located in conjunction with fluorescein leakage than was PED or IRF. IRF was mostly associated with impairment of the neurosensory retina and might represent the earliest manifestation of recurrent CNV^[27-28]. The presence of PED was not associated with fluorescein leakage^[28]; indeed, PED was found irrespective of the occurrence of fluorescein leakage. Instances of nonvascularized PED such as serous or drusenoid PED presented a variety of features of fluorescein status^[29]. Therefore, the presence of PED did not imply active CNV^[26]. The activity of CNV could be evaluated by the

presence of fluid in subretinal, sub-RPE or intraretinal space shown on OCT images^[4,26]. However, fluid could be placed in no CNV lesion. Therefore, multimodal image analysis is required to analyze nAMD exactly because it is initially difficult to diagnose nAMD and to detect the presence of CNV with OCT alone. FA is still the one of gold standard method for diagnosing nAMD.

There were some limitations to this study. First, there was a small number of patients and selection bias due to the retrospective study design. However, enrolled patients had no treatment history of nAMD and received IAI only. The patients with best-corrected visual acuity of less than 20/200 were excluded from this study because they could show fibrotic scar or atrophic change in the macula^[4]. In Korea, treatment-naïve patients, excluding those mentioned here, can receive intravitreal aflibercept or ranibizumab injections, rather than bevacizumab, as insurance system^[30]. Because aflibercept has low injection frequency due to high percentage of fluid absorption and high affinity, it is used more favorably in our clinic^[31]. Therefore, relatively few patients received ranibizumab injection, and this resulted in difficulties or errors in statistical analysis and interpretation, or it was also difficult to sub-analyze. Therefore, we included only patients treated with aflibercept. Also, the patients with polypoidal choroidal vasculopathy were excluded because the segmentation error in OCTA was frequently due to polyps, and patients with retinal angiomatous proliferation were excluded because the size of NV was often too small to be quantitatively analyzed. Therefore, although not many patients were included, the results could be clearly linked to typical nAMD. Second, ICGA was only used to check CNV or not, and to exclude other types than typical nAMD and the features of ICGA were not compared with those of FA or OCTA in this study. There are already several previous studies comparing ICGA and OCTA. Because the characteristics of ICGA and OCTA were similar, such as revealing no dye leakage and demonstrating the entire morphology of CNV, the overlap of lesions in ICGA and OCTA might not yield more meaningful results that FA and OCTA comparisons based on the purpose of the present study. Third, in case of wet AMD with CNV that occurs beneath the RPE layer, FA could not reveal the leakage. However, although CNV was beneath the RPE layer, the features of exudation such as SRF, IRF, and PED were accompanied by disruption of RPE at the CNV and showed hyperfluorescein on FA. Fourth, errors in quantitative analysis of CNV could have occurred because CNV was not completely extracted or choriocapillaries was included in CNV. Some researchers have reported that OCTA shows a slightly lower sensitivity in delineating CNV that occurs beneath the RPE layer^[32]. To overcome this limitation, we tried to correct the

segmentation of OCTA for fully detecting CNV in OCTA and choriocapillaries were removed as much as possible through projection removal and threshold method of software programs used in previous studies.

In summary, the characteristics of CNV were morphologically and quantitatively different according to the leakage status on FA. Tiny capillaries and anastomosis were especially associated with leakage on FA images and changed after treatment. Therefore, it is necessary to carefully examine both the morphological and quantitative changes of CNV on OCTA before and after treatment. By assessing the CNV on OCTA quantitatively and qualitatively, the activity of nAMD is expected even though CNV on OCTA was not completely matched with fluorescein leakage.

ACKNOWLEDGEMENTS

Foundation: Supported in part by the Bio & Medical Technology Development Program of the NRF funded in part by the Korean government and the Ministry of Science and ICT (MSIP; NRF-2017M3A9E2056458; No.2020R1A2C1005729).

Conflicts of Interest: Ahn SM, None; Choi M, None; Yun C, None; Kim SW, None; Oh J, None.

REFERENCES

- 1 Chandra S, Arpa C, Menon D, *et al.* Ten-year outcomes of anti-vascular endothelial growth factor therapy in neovascular age-related macular degeneration. *Eye (Lond)* 2020;34(10):1888-1896.
- 2 Xu D, Dávila JP, Rahimi M, Rebhun CB, Alibhai AY, Waheed NK, Sarraf D. Long-term progression of type 1 neovascularization in age-related macular degeneration using optical coherence tomography angiography. *Am J Ophthalmol* 2018;187:10-20.
- 3 Coscas F, Cabral D, Pereira T, *et al.* Quantitative optical coherence tomography angiography biomarkers for neovascular age-related macular degeneration in remission. *PLoS One* 2018;13(10):e0205513.
- 4 Jaffe GJ, Ying GS, Toth CA, Daniel E, Grunwald JE, Martin DF, Maguire MG, Comparison of Age-related Macular Degeneration Treatments Trials Research Group. Macular morphology and visual acuity in year five of the comparison of age-related macular degeneration treatments trials. *Ophthalmology* 2019;126(2):252-260.
- 5 Coscas F, Lupidi M, Boulet JF, Sellam A, Cabral D, Serra R, François C, Souied EH, Coscas G. Optical coherence tomography angiography in exudative age-related macular degeneration: a predictive model for treatment decisions. *Br J Ophthalmol* 2019;103(9):1342-1346.
- 6 de Carlo TE, Romano A, Waheed NK, Duker JS. A review of optical coherence tomography angiography (OCTA). *Int J Retina Vitreous* 2015;1:5.
- 7 Rofagha S, Bhisitkul RB, Boyer DS, Sadda SR, Zhang K; SEVEN-UP Study Group. Seven-year outcomes in ranibizumab-treated patients in ANCHOR, MARINA, and HORIZON: a multicenter cohort study (SEVEN-UP). *Ophthalmology* 2013;120(11):2292-2299.
- 8 Moshfeghi DM, Thompson D, Saroj N. Changes in neovascular activity

- following fixed dosing with an anti-vascular endothelial growth factor agent over 52 weeks in the phase III VIEW 1 and VIEW 2 studies. *Br J Ophthalmol* 2020;104(9):1223-1227.
- 9 Miere A, Butori P, Cohen SY, Semoun O, Capuano V, Jung C, Souied EH. Vascular remodeling of choroidal neovascularization after anti-vascular endothelial growth factor therapy visualized on optical coherence tomography angiography. *Retina* 2019;39(3):548-557.
 - 10 Al-Sheikh M, Iafe NA, Phasukkijwatana N, Sadda SR, Sarraf D. Biomarkers of neovascular activity in age-related macular degeneration using optical coherence tomography angiography. *Retina* 2018;38(2):220-230.
 - 11 von der Emde L, Thiele S, Pfau M, Nadal J, Meyer J, Möller PT, Schmid M, Fleckenstein M, Holz FG, Schmitz-Valckenberg S. Assessment of exudative activity of choroidal neovascularization in age-related macular degeneration by OCT angiography. *Ophthalmologica* 2020;243(2):120-128.
 - 12 Zeng XM, Hu YJ, Chen YH, *et al*. Retinal neurovascular impairment in non-diabetic and non-dialytic chronic kidney disease patients. *Front Neurosci* 2021;15:703898.
 - 13 Peng QS, Hu YJ, Huang MQ, *et al*. Retinal neurovascular impairment in patients with essential hypertension: an optical coherence tomography angiography study. *Invest Ophthalmol Vis Sci* 2020;61(8):42.
 - 14 Perrott-Reynolds R, Cann R, Cronbach N, *et al*. The diagnostic accuracy of OCT angiography in naive and treated neovascular age-related macular degeneration: a review. *Eye (Lond)* 2019;33(2):274-282.
 - 15 Ma J, Desai, Nesper P, Gill M, Fawzi A, Skondra D. Optical coherence tomographic angiography imaging in age-related macular degeneration. *Ophthalmol Eye Dis* 2017;9:1179172116686075.
 - 16 Choi M, Kim SW, Yun C, Oh J. OCT angiography features of neovascularization as predictive factors for frequent recurrence in age-related macular degeneration. *Am J Ophthalmol* 2020;213:109-119.
 - 17 Takeuchi J, Kataoka K, Ito Y, Takayama K, Yasuma T, Kaneko H, Terasaki H. Optical coherence tomography angiography to quantify choroidal neovascularization in response to aflibercept. *Ophthalmologica* 2018;240(2):90-98.
 - 18 Toth CA, Tai V, Chiu SJ, *et al*, Comparison of Age-Related Macular Degeneration Treatments Trials (CATT) Research Group. Linking OCT, angiographic, and photographic lesion components in neovascular age-related macular degeneration. *Ophthalmol Retina* 2018;2(5):481-493.
 - 19 Costanzo E, Miere A, Querques G, Capuano V, Jung C, Souied EH. Type 1 choroidal neovascularization lesion size: indocyanine green angiography versus optical coherence tomography angiography. *Invest Ophthalmol Vis Sci* 2016;57(9):OCT307-OCT313.
 - 20 Steinle NC, Du WM, Gibson A, Saroj N. Outcomes by baseline choroidal neovascularization features in age-related macular degeneration. *Ophthalmol Retina* 2021;5(2):141-150.
 - 21 de Oliveira Dias JR, Zhang QQ, Garcia JMB, Zheng F, Motulsky EH, Roisman L, Miller A, Chen CL, Kubach S, de Sisternes L, Durbin MK, Feuer W, Wang RK, Gregori G, Rosenfeld PJ. Natural history of subclinical neovascularization in nonexudative age-related macular degeneration using swept-source OCT angiography. *Ophthalmology* 2018;125(2):255-266.
 - 22 Eandi CM, Ciardella A, Parravano M, *et al*. Indocyanine green angiography and optical coherence tomography angiography of choroidal neovascularization in age-related macular degeneration. *Invest Ophthalmol Vis Sci* 2017;58(9):3690-3696.
 - 23 Wang Y, Hu ZL, Zhu TP, *et al*. Optical coherence tomography angiography-based quantitative assessment of morphologic changes in active myopic choroidal neovascularization during anti-vascular endothelial growth factor therapy. *Front Med (Lausanne)* 2021;8:657772.
 - 24 Faes L, Ali Z, Wagner S, Patel PJ, Fu DJ, Bachmann LM, Schmid MK, Waheed N, Keane PA, Balaskas K. Effect of total anti-VEGF treatment exposure on patterns of choroidal neovascularisation assessed by optical coherence tomography angiography in age-related macular degeneration: a retrospective case series. *BMJ Open Ophthalmol* 2019;4(1):e000244.
 - 25 Liang MC, de Carlo TE, Baurnal CR, Reichel E, Waheed NK, Duker JS, Witkin AJ. Correlation of spectral domain optical coherence tomography angiography and clinical activity in neovascular age-related macular degeneration. *Retina* 2016;36(12):2265-2273.
 - 26 Wilde C, Patel M, Lakshmanan A, Amankwah R, Dhar-Munshi S, Amoaku W, Medscape. The diagnostic accuracy of spectral-domain optical coherence tomography for neovascular age-related macular degeneration: a comparison with fundus fluorescein angiography. *Eye (Lond)* 2015;29(5):602-609; quiz 610.
 - 27 Schmidt-Erfurth U, Waldstein SM. A paradigm shift in imaging biomarkers in neovascular age-related macular degeneration. *Prog Retin Eye Res* 2016;50:1-24.
 - 28 Giani A, Luiselli C, Esmaili DD, Salvetti P, Cigada M, Miller JW, Staurenghi G. Spectral-domain optical coherence tomography as an indicator of fluorescein angiography leakage from choroidal neovascularization. *Invest Ophthalmol Vis Sci* 2011;52(8):5579-5586.
 - 29 Tan ACS, Simhae D, Balaratnasingam C, Dansingani KK, Yannuzzi LA. A perspective on the nature and frequency of pigment epithelial detachments. *Am J Ophthalmol* 2016;172:13-27.
 - 30 Jin KW, Kim JH, Park JY, Park SJ, Park KH, Lee JY, Woo SJ. Long-term outcomes of ranibizumab vs. aflibercept for neovascular age-related macular degeneration and polypoidal choroidal vasculopathy. *Sci Rep* 2021;11:14623.
 - 31 Park DH, Sun HJ, Lee SJ. A comparison of responses to intravitreal bevacizumab, ranibizumab, or aflibercept injections for neovascular age-related macular degeneration. *Int Ophthalmol* 2017;37(5):1205-1214.
 - 32 Farecki ML, Gutfleisch M, Faatz H, Rothaus K, Heimes B, Spital G, Lommatzsch A, Pauleikhoff D. Characteristics of type 1 and 2 CNV in exudative AMD in OCT-angiography. *Graefes Arch Clin Exp Ophthalmol* 2017;255(5):913-921.